Alexandr NOVOZHILOV[1], Alexandra POTAPENKO[1] , Timofey NOVOZHILOV[2]

S.Toraygyrov Pavlodar State University(, Republik of Kazakjtan1)
Omsk State University. Russian Federation (2)

doi:10.15199/48.2018.06.06

Process Simulation in Induction Motor where Short-Circuit Rotor Bar is Failed during Run-down Regime

Abstract *In the article is presented a method of modeling processes in a run down regime of an induction motor with a squirrel-cage rotor with broken bars. This method based on the mathematical model of induction motor with a squirrel-cage rotor. Differential equations of this model are composed of mesh current method for line-to-line voltages. This method allows to calculate the harmonic spectrum of current distribution in rotor bars, the rotor speed, the damping coefficient of the currents in the run down regime and the electromotive difference of potential induced in the stator windings, with an accuracy of 10-15%. Results of calculation and experiment are presented in the article.*

Streszczenie. *W artykule opisano modelowanie silnika indukcyjnego z uszkodzonym wirnikiem na etapie zwalniania ruchu. Metoda pozwla obliczać widmo prądu w prętach wirnika, prędkośc wirnika, współczynnik tłumienia prądu oraz potencjał indukowany w uzwojeniu stojana. Wyniki obliczrń porównano z danymi eksperymentalnymi.* ***Symulacja silnika indukcyjnego z uszkodzonym wirnikiem podczas zwalniania ruchu***

Keywords: diagnostic system of rotor, mathematical model of the induction motor, run down regime, broken rotor bars.
Słowa kluczowe: diagnostyka, silnik indukcyjny, uszkodzenie wirnika

Introduction

Damages from operation of an induction motor (IM) with a short-circuit rotor when its bars are broken are mainly expressed in increased power consumption [1]. At the same time, the cost of power over consumption for the year of operation of such IM often exceeds the cost of engine itself[2]. Due to this fact there are many proposals on how to diagnose this type of damage during operation[3,10-23]. However most of them cannot be realized because of the effect of electric network parameters fluctuations, IM vibrations and resistance moment variation load on the measured signal. These effects can be ignored if IM diagnosis is carried out during run-down regime[3, 24-25]. However under these conditions development of such a diagnostic system without process simulation in IM is impossible.

IM run-down regime starts when it is disconnected from the power network. Immediately after IM switching off the currents in stator winding become equal to zero and currents in rotor winding remain the same as they were at the moment of shutdown. Thereafter due to the fact that active resistances are available in the rotor windings attenuation of them occurs. At the same time speed of rotor rotation slows down under the impact of resistance moment in IM bearings, its air fan and drive mechanism. As a result EMF is changed in stator windings not only in terms of magnitude but in frequency.

Mathematical model of induction motor

In order to simulate processes occurring when IM runs-down with a broken rotor bar it is convenient to use a mathematical model differential equations of which are compiled by the method of loop currents for phase-to-phase voltages[4]. According to this mathematical model, taking into account Fig. 1 (K keyswitch closed) and application

$$(1)\quad \left.\begin{aligned} u_{AB} &= (R_A + R_B)i_1 - R_B i_2 + d\psi_1/dt; \\ u_{BC} &= (R_B + R_C)i_2 - R_B i_1 + d\psi_2/dt; \\ 0 &= (R_a + R_b)i_3 - R_b i_4 + d\psi_3/dt; \\ 0 &= (R_b + R_c)i_4 - R_b i_3 + d\psi_4/dt, \end{aligned}\right\}$$

where instantaneous values u_{AB} u_{BC} of phase-to-phase voltages; instantaneous values $i_1 \div i_4$ of loop currents; - instantaneous values i_A, i_B, i_C and i_a, i_b, i_c of currents in phases of stator and rotor windings; instantaneous values $i_1 \div i_4$ of currents in circuits; R_A, R_B, R_C и R_a, R_b, R_C - active resistance of stator and rotor windings; $\psi_1 \div \psi_4$ contours linkage [4].

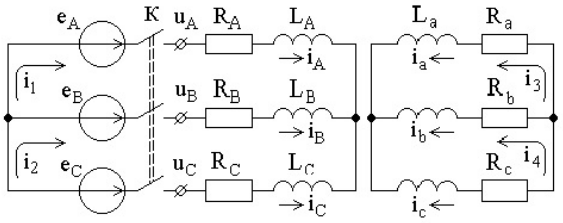

Fig.1. Distribution of currents in IM windings.

The equations of moments and rotor motion in this model are the mathematical expressions

$$(2)\quad M_q = \sum_{k=1,2} i_k \sum_{n=3,4} i_n \frac{d L_{kn}}{d \alpha_{kn}};\ j\frac{d\omega_2}{dt} = M_c + M_q,$$

where M_q - electromagnetic moment is IM; M_c - resistance moment of drive mechanism and IM; L_{kn} - mutual inductance of contours which are calculated by [4]; J- total inertia moment of IM rotor and drive mechanism rotation; k and n numbers of stator and rotor circuits; ω_2 - angular rotational speed of the rotor.

As a result, when IM is disconnected at a point of time t the currents in stator and rotor windings are defined in the following way.

(3) $i_A = i_1$, $i_B = i_2 - i_1$, $i_C = -i_2$, $i_a = i_3$, $i_b = i_4 - i_{31}$, $i_c = -i_4$.

If it was running in an arbitrary and stationary operational way when IM was disconnected the currents in its windings have only a periodic component which is sought as a particular solution of the system of inhomogeneous equations obtained from (1). Voltages in this system are sinusoidal and differentiation operator d/dt is replaced by $j\omega$. As a result:

$$(4)\quad \left.\begin{aligned} \dot{U}_{AB} &= [(R_A+R_B)+jX_{11}]\dot{I}_1+(-R_B+jX_{12})\dot{I}_2+jX_{13}\dot{I}_3+jX_{14}\dot{I}_4;\\ \dot{U}_{BC} &= (-R_B+jX_{21})\dot{I}_1+[(R_B+R_C)+jX_{22}]\dot{I}_2+jX_{23}\dot{I}_3+jX_{24}\dot{I}_4;\\ 0 &= jX_{31}\dot{I}_1+jX_{32}\dot{I}_2+[(R_a+R_b)+jX_{33}]\dot{I}_3+(-R_b+jX_{34})I_4;\\ 0 &= jX_{41}\dot{I}_1+jX_{42}\dot{I}_2+(-R_b+jX_{43})\dot{I}_3+[(R_a+R_b)+jX_{44}]\dot{I}_4, \end{aligned}\right\}$$

where inductances are calculated as $X_{vw}=\omega L_{vw}$ taking into account (1) and applications and v and w take values from one to four.

IM operation is determined by resistances R_a and R_b which like in equivalent circuits are determined by motor slip. In this case, considering (3) and [5] an amplitude value of the current in bar of the "squirrel cage"

$$(5)\qquad i_{cm}=2I_{3m}\,k_I\,\sin\frac{\pi p}{z_2}$$

where I_{3m} - amplitude value of the current in rotor phase A of the reduced IM; k_I - index of reduction; p- number of IM terminal pairs; z_2 - Number of bars in rotor winding

Simulation of currents in IM during run-down regime is carried out according to the scheme in Fig. 1 where key switch K is open. As a result currents in stator winding become equal to zero and system of equations (1) considering application is transformed into

$$(6)\qquad \left.\begin{aligned} 0 &= i_3(R_a+R_b)-i_4R_b+d\psi_3/dt,\\ 0 &= (i_4-i_3)R_b+i_cR_c+d\psi_4/dt. \end{aligned}\right\},$$

where $\psi_3=i_3L_{33}+i_4L_{34}$ and $\psi_4=i_3L_{43}+i_4L_{44}$; L_{33} and L_{44} internal inductances of rotor circuits; L_{34} and L_{43} - mutual inductances of rotor circuits.

When stator winding currents are equal to zero electromagnetic moment of IM M_q is also equal to zero. In this case equation of rotor motion is the mathematical expression.

$$(7)\qquad j(d\omega_2/dt)=M_c.$$

The damped currents i_3 and i_4 in rotor circuits induce EMF in stator windings value of which, for example, can be determined for phases A and B from the first equation of system (1). As a result considering application

$$(8)\qquad e_{AB}=d\psi_1/dt$$

In case of a numerical solution of a system of equations (6-8) time of investigated process is divided into time by duration Δt. It is believed that within each time intervals i_3, i_4 and ω_2 are unchanged. When changing from time interval q to time interval $q+1$ these values are calculated using formulas below.

In order to determine currents in each time interval system of equations (6) is transformed. Components of voltage drops at active resistances are transferred to the left-hand side of equations and dt and di are replaced by Δt and Δi. As a result change of currents Δi in circuit elements over a time interval Δt will be determined from the system

$$(7)\qquad \left.\begin{aligned} [R_b i_4-(R_a+R_b)i_3]\Delta t &= L_{33}\Delta i_3+L_{34}\Delta i_4;\\ [R_b i_3-(R_b+R_c)i_4]\Delta t &= L_{43}\Delta i_3+L_{44}\Delta i_4. \end{aligned}\right\}$$

Since the currents in rotor circuits are known at the time of IM disconnection their value in interval $q+1$ is defined as

$$(8)\qquad i_{3,q+1}=i_{3,q}+\Delta i_{3,q} \text{ и } i_{4,q+1}=i_{4,q}+\Delta i_{4,q}.$$

Accuracy of calculation is affected by correctness of the choice Δt. On the one hand reduction Δt should lead to increase in the accuracy of calculation. On the other hand Δt reduction leads to number increase in matrix calculations (7) and accuracy of current detection depends on capabilities of computer software.

Fig. 2 shows calculated attenuation of currents i_3 and i_4 in rotor winding of the reduced IM 4AM100L6Y3 at Δt = 0.00025s.

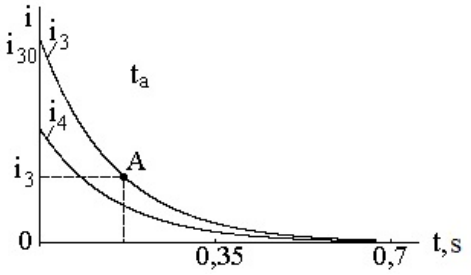

Fig. 2. Attenuation of current in rotor winding under IM 4AM100L6Y3 run-down regime

Considering Fig. 2 and [6] the nature of attenuation, for example, current i_3 can be described as

$$(9)\qquad i_3=i_{30}\,e^{-kt_a},$$

where $k=ln(i_3/i_{30})/t_a$ - attenuation coefficient.

Obviously, current i_4 and currents in bars of the rotor "squirrel cage" are attenuated in a similar way.

Currents i_3 and i_4 in reduced rotor winding of an intact IM during shutdown meet a sinusoidal distribution of current values in bars of the "squirrel cage" along the air gap [5]. It is for IM with p = 3 in Fig. 3 and shown by a dashed line. Such distribution of current values along rotor bars rotating with angular velocity $\omega_2=\omega_1(1-s)$ induces EMF $E_{AB,0}$ with frequency $f_2=\omega_2/2\pi$ in phases A and B where ω_1 is the angular velocity of stator rotation magnetic field; s - sliding of rotor [5]. The spectral analysis $E_{AB,0}$ is shown in Fig. 3b also by a dash line [7].

When n_c^* bar is broken the current becomes equal to zero in it. In this case value of currents in bars against of it increases as shown in Fig. 3b by thick lines [7,8]. Such distribution of current values along bars of rotating rotor is not sinusoidal (Figure 3 a, solid lines) and induces not only the main EMF $E_{AB,0}$ with frequency f_2 but also additional EMF $E_{AB,d1}$ and $E_{AB,d2}$ with frequencies in windings of phase A and B and stator.

$$(10)\qquad f_{d1}=f_2(1-1/p)\;;\; fd=f_2(1+1/p).$$

EMF value for the q-th time interval, for example, phases A and B, can be determined from the first system equation (1) as

$$(11)\; e_{AB,q}=\Delta\psi_{1,q}/\Delta t=(\Delta i_{3,q}L_{13}+\Delta i_{4,q}L_{14})/\Delta t\;,$$

where L_{13} and L_{14} - mutual inductances of stators and rotor circuits.

Rotor speed rotation is slowed down for time interval $q+1$ considering (7), it is defined as

(12) $$\omega_{2,q+1} = \omega_{2,q} + M_{сн}(\frac{\omega_{2,q}}{\omega_{2н,q}})^g \frac{\Delta t}{J},$$

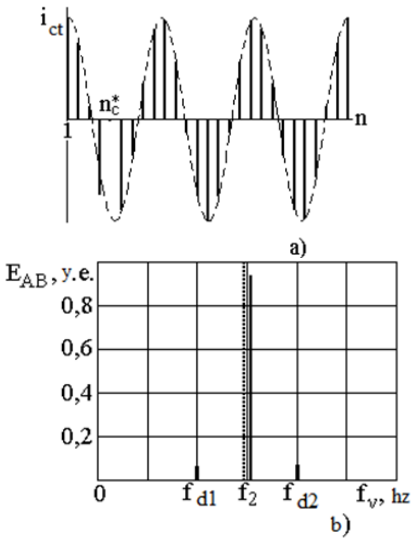

Fig. 3. Currents distribution in "squirrel cage" bars of IM 4AM100L6Y3 rotor when the fifth bar is broken during offload and EMF induction by it in phases A and B of the stator

where $M_{сн}$ - nominal resistance moment at the moment of IM disconnection at $\omega_{2н}$ nominal angular rotational speed of the rotor; g - index of degree which can be taken equal to two for traction and blowing mechanisms as well as bearings [9].

Thus, if the attenuation index k, distribution of currents in the "squirrel cage" bars and change of rotor rotation speed during run-down regime are known EMF of stator phases A and B can be defined at any time t as:

(14) $$e_{AB}(t) = e_{AB,0}e^{-kt}\cos(\omega_2 t + p\gamma) + e_{AB,d1}e^{-kt}\cos[\omega_2 t + (p+1)\gamma] + e_{AB,d2}e^{-kt}\cos[\omega_2 t + (p-1)\gamma]$$

where $e_{AB,0}$, $e_{AB,d1}$ and $e_{AB,d2}$ is EMF induced by current distribution components in the "squirrel cage" bars with frequencies f_0, f_{d1} and f_{d2} accordingly;

$\gamma = \gamma_0 + \int_0^t \omega_2 dt$ - angle between axis of the stator phase A and axis of the rotor phase a; γ_0 is an initial angle between axis of the stator phase A and axis of the rotor phase a.

The results of modeling

Simulation results shown in EMF oscillograms of stator IM 4AM100L6Y3 phases A and B during run-down regime from off-load at Δt=0.00025 s are shown in Fig. 7. Comparing results obtained in spectral analysis of oscillograms as a result of simulation and experiment has shown that inaccuracy in EMF simulation induced on terminals of stator winding does not exceed 10-15%.

Experiments

The experimental results of the IM 4AM100L6Y3 are shown in Figures 2 and 3 in the form of dependences

(14) $$E_1^* = E_1 / U_1,\ E_{1-1/p}^* = E_{1-1/p} / E_{(1-1/p),н},$$

where $E_{(1-1/p),н}$ - is EMF of an additional harmonic at the initial of running-down.

In this case, lines 1 and 2 represent these dependences for the sound and impaired rotor. It can be seen from Figures 4 and 5 that the damping of the EMF $E_p(t)$ and $E_{p-1}(t)$ when running-down is in the same manner. This allows us to use the ratio of $\sigma_{1-1/p} = E_{1-1/p} / E_1$ as an identification feature of the breakage of the rotor bars in the run-down regime of IM.

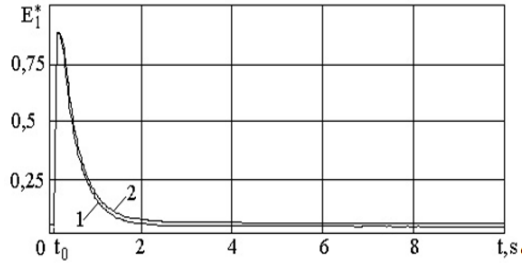

Fig.4 Oscillogram of the first harmonic of the EMF in the stator winding of the sound and impaired IM 4AM100L6Y3 in the run-down regime

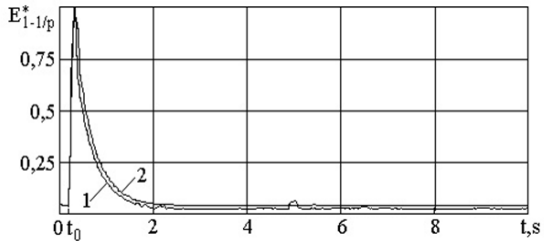

Fig5. - Oscillogram of one of the additional EMF of the stator winding of the sound and impaired IM 4AM100L6Y3 in the run-down regime

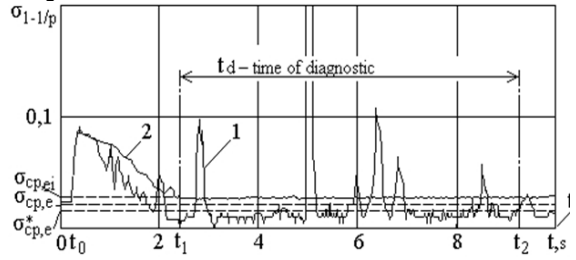

Fig.6- Dependencies for the sound and impaired IM 4AM100L6Y3 in the run-down regime

First of all, the bandwidth for diagnosis limited by time t_1 and t_2 is to be determined. Then for this bandwidth the average value $\sigma_{cp,e}$ of the dependence $\sigma_{(1-1/p),e}(t)$ is calculated and the adjusted dependence $\sigma^*_{(1-1,p),e}(t)$ is derived. Further, for the adjusted dependence $\sigma^*_{(p-1),e}(t)$, an average adjusted value $\sigma^*_{cp,e}$ of this dependence is determined. In the future, it is used to clarify the results of the success diagnosis of IM.

Figure 6 shows that in the interval of time $t_1 \div t_2$ the ratio $\sigma_{p-1}(t)$ for IM, with the exception of a few jumps, is relatively stable. In this interval t_1 is determined by the time at which the EMF in the stator winding from the currents in the rotor winding becomes commensurable with the EMF induced by the magnetized magnetic core of the rotor. In this regard, the time can be determined with sufficient

accuracy in relation to where and is the EMF at the time t_1 can be accurately determined using formula $\sigma_{t_1} = E_{1,t_1} / E_{1,t_0}$, where E_{1,t_0} E_{1,t_1} - EMF E_1 at the moment of disconnection and beginning of the diagnosis of the IM. From numerous experiments with the IM with a different number of pole pairs and power, it was possible to find out that the value σ_{t_1} should be taken equal to 0.065-0.075.

The average value $\sigma_{cp,e}$ of the dependency $\sigma_{(1-1/p),e}(t)$ during the time of diagnosis when processing a signal under the Short Time Fourier Transform is defined as ..

$$\sigma_{cp,e} = \sum_{n=1}^{N} \sigma_{(p-1),e} / N , \quad (15)$$

where the time interval of the diagnostic zone is represented by $N = (t_2 - t_1)/\Delta t$ points at the window pitch Δt equal to the time of one period.

The average value $\sigma_{cp,e}$ for the IM 4AM100L6Y3 with the sound winding of the rotor in Figure 6 is shown in dotted line. Comparison of the value $\sigma_{cp,e}$ and the dependence $\sigma_{p-1}(t)$ in Figure 6 shows that the dependences $\sigma_{(1-1/p),e}(t)$ of the IM 4AM100L6Y3 are characterized by significant jumps in magnitude relative to $\sigma_{cp,e}$. In this connection, the dependence $\sigma_{p-1}(t)$ is adjusted.

To do this, all values $\sigma_{(1-1/p),e} > \sigma_{cp,e}$ are replaced by $\sigma_{(1-1/p),e} = \sigma_{cp,e}$. Next, according to the adjusted dependence $\sigma^*_{(p-1),e}(t)$ the average adjusted value is determined

$$\sigma^*_{cp,e} = \sum_{n=1}^{N} \sigma^*_{(p-1),e} / N , \quad (16)$$

which is also shown in Figure 6 by the dotted line.

As a rule, the average adjusted value $\sigma^*_{cp,u}$ can be used as the first criterion for estimating the state of the rotor winding.

At the same time, the average adjusted value $\sigma^*_{cp,ei}$ calculated in a similar way from the dependence $\sigma_{(1-1/p),ei}(t)$ obtained for the IM with the impaired rotor can be used as the second criterion for estimating the state of the rotor winding.

Taking into account these criteria and Figure 6, it becomes clear that as an identification feature of the fault in the allocated time interval, one can use the ratio

$$k_\varepsilon = \sigma_{cp,ei} / \sigma^*_{cp,e} . \quad (17)$$

It can be seen from Figure 6 that when one bar is broken, the k_ε of the IM 4AM100L6Y3 is 1.8-2.0. That allows reliable determining of the breakage of one bar in the winding of the rotor.

Conclusion

1. Bar failure in short-circuit winding of induction motor rotor during run-down regime leads to EMF stator appearance with frequency f_2 induced additional EMFs with frequencies $f_2(1 \pm 1/p)$ by currents in rotor winding.
2. The EMFs induced in stator windings when induction motor runs-down are proportional to currents in rotor winding and its frequency is the rotational speed of rotor.
3. The currents in rotor winding during run-down regime decay exponentially, while the decay time is the greater the smaller value of "squirrel cage" active resistances elements.
4. Rotor rotation speed during run-down regime depends on moment of rotor inertia and resistance moment and.
5. The use of the value k_ε as an identification feature of the breakage of the rotor bars is fully justified.

Appendix 1.

Flux linkage and inductance of IM mathematical model [4]. Resulting circuits flux linkages:

$$\psi_1 = L_{11} i_1 + L_{12} i_2 + L_{13} i_3 + L_{14} i_4 ,$$
$$\psi_2 = L_{21} i_1 + L_{22} i_2 + L_{23} i_3 + L_{24} i_4 ,$$
$$\psi_3 = L_{31} i_1 + L_{32} i_2 + L_{33} i_3 + L_{34} i_4 ,$$
$$\psi_4 = L_{41} i_1 + L_{42} i_2 + L_{43} i_3 + L_{44} i_4 .$$

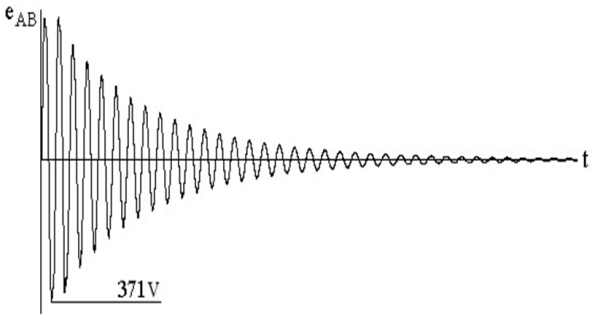

Fig. 7. The calculated EMF values in stator winding of IM 4AM100L6Y3 after disconnection from the network.

Own inductance circuits:

$$L_{11} = L_A - 2L_{AB} + L_B ; \quad L_{22} = L_B - 2L_{BC} + L_C ;$$
$$L_{33} = L_a - 2L_{ab} + L_b ; \quad L_{44} = L_b - 2L_{bc} + L_c$$

Mutual circuits inductance:

$$L_{12} = L_{AB} - L_B - L_{AC} + L_{BC} = L_{21} ,$$
$$L_{23} = L_{Ba} - L_{Ca} - L_{Bb} + L_{Cb} = L_{32} ,$$
$$L_{13} = L_{Aa} - L_{Ba} - L_{Ab} + L_{Bb} = L_{31} ,$$
$$L_{24} = L_{Bb} - L_{Cb} - L_{Bc} + L_{Cc} = L_{42} ,$$
$$L_{14} = L_{Ab} - L_{Bb} - L_{Ac} + L_{Bc} = L_{41} ,$$
$$L_{34} = L_{ab} - L_b - L_{ac} + L_{bc} = L_{43}$$

The main inductances of all phase windings are the same and do not depend on the angular position of rotor in the machine above.

$$L_{Am} = L_{Bm} = L_{Cm} = L_{am} = L_{bm} = L_{cm} = L_m = \frac{4\mu_0}{p\pi^2} w_1^2 k_{01}^2 \frac{\tau l_\delta}{\delta l_\delta} , \text{w}$$

here L_m - maximum reduced mutual inductance between stator and rotor; w_1 and k_{01} -number of coils in stator winding and its winding index; τ- pole pitch; l_δ - thickness

of stator core with no ventilation ducts; δ - air gap size; k_δ - Carter coefficient.

The main inductances between stator and rotor phases also do not depend on the angular position of rotor and are defined as

$$L_{ABm} = L_{BCm} = L_{CAm} = L_{abm} = L_{bcm} = L_{cam} = -L_m / 2$$

Self-inductances of stator and rotor phases:

$$L_A = L_{Am} + L_{A\delta},$$
$$L_a = L_{am} + L_{a\delta},$$
$$L_B = L_{Bm} + L_{B\delta},$$
$$L_b = L_{bm} + L_{b\delta},$$
$$L_C = L_{Cm} + L_{C\delta},$$
$$L_c = L_{cm} + L_{c\delta}.$$

Mutual inductances between stator and rotor phases:

$$L_{AB} = L_{ABm} + L_{AB\delta},$$
$$L_{ab} = L_{abm} + L_{ab\delta},$$
$$L_{BC} = L_{BCm} + L_{BC\delta},$$
$$L_{bc} = L_{bcm} + L_{bc\delta},$$
$$L_{CA} = L_{CAm} + L_{CA\delta},$$
$$L_{ca} = L_{cam} + L_{ca\delta}.$$

These mathematic expressions the highest harmonics air gap are marked with index "δ"which are considered only when calculating inductances and mutual leakage inductances.

Only mutual inductances between phases of stator and rotor depend on the angular position of rotor determined by the value of angle γ between axes A and a.

$$L_{Aa} = L_{Bb} = L_{Cc} = L_m \cos\alpha_{Aa}, \qquad \alpha_{Aa} = p\gamma,$$
$$L_{Ac} = L_{Ba} = L_{Cb} = L_m \cos\alpha_{Ac}, \qquad \alpha_{Ab} = p\gamma + 2\pi/3,$$
$$L_{Ab} = L_{Bc} = L_{Ca} = L_m \cos\alpha_{Ab}, \qquad \alpha_{Ac} = p\gamma + 4\pi/3.$$

Authors: *Novozhilov, Aleksandr Nikolaevich, S. Toraighyrov E-mail: novozhlov@bk.ru,*
Potapenko Alexandra Olegovna E-mail: alxopt@gmail.com.
Novozhilov, Timofey Aleksandrovich Omsk State University as a post-graduate student.

REFERENCES

[1] Yermolin N.P., Zherikhin I.P. Nadezhnost electricheskikh mashin [Reliability of power machines]. - L.: Energiya, 1976.- 247c.

[2] Novozhilov A.N., Kislov A.P., Andreyeva O.A. Energopotrebleniye assinkhronnogo dvigatelya pri obryve sterzhney i ekstsentrissitite korotkozamknutogo rotora [Power Consumption of an Induction Motor when Bars and Eccentricity of Short-Circuit Rotor are Failes].//Bulletin of PSU, Power serie. - 2003, - №4. - c.23-28.

[3] Novozhilov A.N., Potapenko A.O. Novozhilov T.A. Metody diagnostiki obryva sterzhney korotkozamknutogo rotora assinkhronnogo dvigatelya [Methodics to Diagnose Failure of Bars in Short-Circuit Rotor of an Induction Motor] //Bulletin of PSU. Power serie. - 2015, - №1. - c.120-129.

[4] Novozhilov A.N. Matematicheskoye modelirovaniye ekspluatatsionnykh i avariinykh rezhimov raboty assinkhronnykh dvigateley [Mathematic Simulation of Operational and Emergency Operations for Induction Motors] // Elektrichestvo. – 2000.- №5.- C.37÷41.

[5] Ivano-Smolenskiy A.V. Elektricheskiye mashiny [Power Machines]. -M.: Energiya. 1980.- 909c.

[6] Bessonov L.A. Teoreticheskiye osnovy elektrotekhniki [Theoretical Science of Electric Engineering]. -M.: Vysshaya Shkola. 1967.- 775c.

[7] Novozhilov A.N., Potapenko A.O. Metod modelirovaniya tokov v assinkhronnom dvigatele pri povrezhdenii "belichyey kletki"; [Method of Current Simulation in an Induction Motor when "squirrel cage" failed]//Bulletin of PSU, Power serie. - 2014, - №4. - c.95-100.

[8] Boguslavskiy I.Z. Toki v nessimetrichnoy korotkozamknutoy kletke rotora [Currents in Asymmetrical Short-Circuit Cage of Rotor]//Power Engineering and Transport. The News of the ASUSSR. - 1982.-№1.- C. 71÷76.

[9] Syromyatnikov I.A. Rezhimy raboty assinkhronnykh I sinkhronnykh dvigateley [Operation of Induction and Synchronous Motors]. -M.: Energoatomizdat. 1984.- 240c.

[10]Faiz, J. , B.-M. , Ebrahimi A new pattern for detecting broken rotor bars in induction motors during start-up , *IEEE Trans. Magn.*, (2008), No. 12 , 4673-4683.

[11]Talhaoui, H., Menacer, A., Kessal, A., Kechida, R. Fast Fourier and discrete wavelet transforms applied to sensorless vector control induction motor for rotor bar faults diagnosis, ISA Transactions, (2014), No 53, 1639–1649.

[12] Pineda-Sanchez, M., M.Riera-Guasp, J. A. Antonino-Daviu, J. Roger-Folch, J. Perez-Cruz, and R. Puche-Panadero, Instantaneous frequency of the left sideband harmonic during the start-up transient a new method for diagnosis of broken bars, *IEEE Trans. Ind. Electron,* (2009), No. 11, 4557-4570.

[13] Luis, A., Garcна-Escudero, Oscar Duque-Perez, Morinigo-Sotelo,D., Perez-Alonso, M. Robust condition monitoring for early detection of broken rotor bars in induction motors, Expert Systems with Applications, (2011), No 38, 2653–2660.

[14] Akar, M. Detection of rotor bar faults in field oriented controlled induction motors, Journal of Power Electronics, (2012), 1-9.

[15] Didiera, G., Ternisienb, E., Casparyb, O., Razika H. A new approach to detect broken rotor bars in induction machines by current spectrum analysis, Mechanical Systems and Signal Processing, (2007), No 21, 1127–1142.

[16] Karamia, F., Poshtan, J., Poshtan, M. Detection of broken rotor bars in induction motors using nonlinear Kalman filters, ISA Transactions, (2010), No49, 189-195.

[17] Shuo Chen, Zivanovic, R. Modelling and simulation of stator and rotor fault conditions in induction machines for testing fault diagnostic techniques, Euro. Trans. Electr. Power, (2010), No20, 611–629.

[18] Harris, F. On the Use of Windows for Harmonic Analysis with the Discrete Fourier Transform, IEEE, (1978), No66 (1), 51-83.

[19] Smail Bachir, Slim Tnani, Jean-Claude Trigeassou, & Gérard Champenois Diagnosis by Parameter Estimation of Stator and Rotor Faults Occurring in Induction Machines, IEEE Transaction on industrial electronics, (2006), No53 (3), 963-973.

[20] Barut, M. Bi Input-extended Kalman filter based estimation technique for speed-sensorless control of induction motors, Energy Conversion and Management, (2010) No51, 2032–2040.

[21] Kia, S., Henao, H., Capolino,G-A. A High-Resolution Frequency Estimation Method for Three-Phase Induction Machine Fault Detection, IEEE Transaction on industrial electronics, (2007), No54(4), 2305-2314.

[22] Aderiano, M., Povinelli, R., Nabeel, A. Demerdash Induction Machine Broken Bar and Stator Short-Circuit Fault Diagnostics Based on Three-Phase Stator Current Envelopes, IEEE Transaction on industrial electronics, (2008), No 55 (3), 1310-1318.

[23] Nandi, S., Bharadwaj, R., Toliyat, H., Parlos, A. Study of three-phase induction motors with incipient rotor cage faults under different supply conditions, IEEE-IAS, (1999), No 3, 1922–1928.

[24] Kalinov, A.P., Ukhan, Zh.I., Urdin, I.V. Diagnostic methods for detection of rotor bar damage, KDPU newsletter. Col. of sc. papers of KDPU named after M. Ostrogradskiy, (2009), No4(57), 98-101

[25] Romashikhina, Zh.I., Kalinov, A.P., Application of wavelet analysis for detection of winding bar breakage of induction motors, Electromechanical and energy-saving systems, (2010) No 12, .22-27